Available online at www.sciencedirect.com
ScienceDirect
ELSEVIER
Polymer 48 (2007) 3429–3436
polymer
www.elsevier.com/locate/polymer

Morphological architecture of poly(*p*-oxybenzoyl) by modification of oligomer end-group

Kunio Kimura*, Yasuhiro Kurihara, Hideki Omori, Shin-ichiro Kohama, Shinichi Yamazaki, Yuhiko Yamashita

Graduate School of Environmental Science, Okayama University, 3-1-1 Tsushima-naka, Okayama 700-8530, Japan

Received 30 December 2006; received in revised form 20 March 2007; accepted 15 April 2007
Available online 19 April 2007

Abstract

Influence of oligomer end-group on morphology of poly(4-oxybenzoyl) (POB) was examined by polymerizations of 4-acyloxybenzoic acids having different acyl groups. Polymerizations of 4-propionyloxybenzoic acid, 4-hexanoyloxybenzoic acid, 4-octanoyloxybenzoic acid and 4-decanoyloxybenzoic acid in liquid paraffin at 320 °C yielded needle-like or pillar-like POB crystals via crystallization of oligomers. On the other hand, the polymerization of 4-perfluorooctanoyloxybenzoic acid (FOBA) afforded microspheres having needle-like crystals on the surfaces. At an initial stage in the polymerization, microspheres having smooth surface were formed via liquid–liquid phase separation of oligomers prepared from FOBA owing to the low miscibility of perfluorooctanoyl end-group. Thereby the phase-separation behaviour of oligomers changed from liquid–liquid phase separation to crystallization at a middle stage in the polymerization and then needle-like crystals were formed on the surface of the microspheres. Chemical structure of the oligomer end-group affected significantly the phase-separation behaviour of oligomers and ultimately the morphology of POB.

Keywords: Morphology; Polyesters; Phase separation

1. Introduction

Development of rigid-rod aromatic polymers has been an objective of many researches because they are expected as advanced materials due to excellent properties derived from their rigid structures, such as thermal stability, high modulus, solvent resistance and so on [1]. Rigid-rod aromatic polymers are generally infusible and insoluble, and hence it is quite difficult not only to process but also to synthesize them.

POB, which is an intractable aromatic polyester, was prepared by thermal condensation of 4-acetoxybenzoic acid (ABA) in inert aromatic solvents such as Therminol® or Marlotherm-S® [2–7]. Slab-like POB crystals were prepared by the polymerizations in the inert solvents. POB whiskers were successfully prepared by the polymerization of ABA in liquid paraffin (LPF) at a very low concentration without stirring [8,9]. The polymer molecules were aligned along the long axis of the whiskers. The POB whiskers were formed by the reaction-induced crystallization of oligomers with the spiral growth of oligomer lamellae and the subsequent solid-state polymerization in the crystals. These results provided a new method for morphology control of rigid polymers and many other whiskers have been prepared so far [10–16].

The reaction-induced phase separation of oligomer is of great importance to control the morphology, and the miscibility between the oligomer and the solvent determines the phase separation. The miscibility between the oligomer and the solvent is strongly influenced by many factors including the chemical structures of the oligomer and the solvent. Among the chemical structures of the oligomer, it is expected that end-group affected the miscibility leading to the control of the morphology of POB. This paper elucidates the influence

---

* Corresponding author. Tel./fax: +81 86 251 8902.
E-mail address: polykim@cc.okayama-u.ac.jp (K. Kimura).

0032-3861/$ - see front matter © 2007 Elsevier Ltd. All rights reserved.
doi:10.1016/j.polymer.2007.04.025

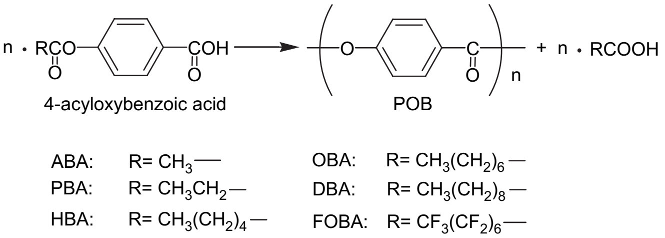

Scheme 1. Polymerization of 4-acyloxybenzoic acids.

of the chemical structure of oligomer end-group on the morphology of POB by using the polymerization of 4-acyloxybenzoic acids having different acyl groups as shown in Scheme 1.

2. Experimental section

2.1. Materials

4-Hydroxybenzoic acid and ABA were purchased from TCI Co. Ltd. 4-Hydroxybenzoic acid was purified by recrystallization from methanol. ABA was purified by recrystallization from ethyl acetate. 4-Propionyloxybenzoic acid (PBA) [6,17], 4-hexanoyloxybenzoic acid (HBA) [6], 4-octanoyloxybenzoic acid (OBA) [18], and 4-decanoyloxybenzoic acid (DBA) [18,19] were synthesized according to the previous procedures. Phenyl 4-hydroxybenzoate was purchased from Aldrich Co. Ltd. and used as received. Perfluorooctanoyl chloride was purchased from PCR Inc. and used as received. 4-(4-Acetoxybenzoyloxy)benzoic acid (ABA dimer) and 4-[4-(4-acetoxybenzoyloxy)benzoyloxy]benzoic acid (ABA trimer) were synthesized according to the previous procedures [20]. LPF was purchased from Nacalai Tesque Co. Ltd and purified by vacuum distillation (220–240 °C/0.3 mmHg).

2.2. Measurements

Morphology of the products was observed on a Hitachi S-2150 scanning electron microscope. Samples were dried, sputtered with gold and observed at 20 kV. IR spectra were measured on a JASCO FT-IR-410 spectrometer. NMR spectra were measured on a JEOL AL300 SC-NMR spectrometer operating at 300 MHz (^{1}H) and 283 MHz (^{19}F). Wide angle X-ray scattering (WAXS) was conducted on a Rigaku 4012K2 with nickel-filtered Cu Kα radiation at 30 kV and 20 mA with a scanning rate of 1°/min.

Number-average degree of polymerization (DPn) was determined as follows: polymers or oligomers (10 mg) and 1 ml of 7.0 wt% KOH methanol solution were placed in a test tube, and kept at 25 °C for 24 h until the sample was completely hydrolyzed. The solution was neutralized with dilute hydrochloric acid and then analyzed by using Shimadzu GC-14B gas chromatography with FID equipped with a Thermon-3000 (60–80 mesh) packed column. DPn was calculated with the molar ratio of 4-hydroxybenzoic acid and the corresponding aliphatic acids derived from end-group.

Concentration–temperature ($C-T$) phase diagram of oligomer model compound–LPF systems was prepared as follows: oligomer model compound and LPF were put into glass tubes at different concentrations. They were placed into an oil bath and heated until the oligomer model compound was entirely dissolved. Then temperature was gradually lowered at a cooling rate of 5 °C h^{-1} and cloud point temperature was determined. The phases and conjugate line between liquid and solid phases were confirmed on a Yanaco MP-500D microscope equipped with a heating stage under crossed polarization.

2.3. Synthesis

FOBA: into a flask equipped with a dropping funnel, a thermometer and a gas inlet tube were placed 4-hydroxybenzoic acid (3.00 g, 21.7 mmol), triethylamine (4.84 g, 47.7 mmol) and 20 ml of dried tetrahydrofuran. Solution of perfluorooctanoyl chloride (9.39 g, 21.7 mmol) in 10 ml of dried tetrahydrofuran was added dropwise through the dropping funnel under slow stream of nitrogen at 5 °C. Temperature was kept at 5 °C for 2 h and then at 25 °C for 12 h. The reaction mixture was filtrated to separate triethylamine–HCl salts and acidified by diluted HCl solution. White precipitates were collected and washed with water. Recrystallization from a mixture of toluene and *n*-hexane gave 3.95 g (77%) of FOBA crystals. Purity was checked by HPLC. Tm: 153 °C. IR (KBr, cm^{-1}): 3300–2500 (OH), 3080 (aromatic C–H), 1785 (ester C=O), 1700 (carboxylic acid C=O), 1245 (aliphatic C–F). ^{1}H NMR (DMSO-d_6, ppm): $\delta = 7.48$ (d, aromatic, 2H), 8.07 (d, aromatic, 2H), 12.69 (s, carboxylic acid, 1H). ^{19}F NMR (DMSO-d_6, ppm): $\delta = -120.35$ ($CF_3{-}C\mathit{F}_2{-}$, 2F), -117.03 ($CF_3{-}CF_2{-}C\mathit{F}_2{-}$, 2F), -116.93 ($CF_3{-}CF_2{-}CF_2{-}C\mathit{F}_2{-}$, 2F), -116.32 ($CF_3{-}CF_2{-}CF_2{-}CF_2{-}C\mathit{F}_2{-}$, 2F), -116.04 ($CF_3{-}CF_2{-}CF_2{-}CF_2{-}CF_2{-}C\mathit{F}_2{-}$, 2F), -113.11 ($CF_3{-}CF_2{-}CF_2{-}CF_2{-}CF_2{-}CF_2{-}C\mathit{F}_2{-}COO{-}$, 2F), -74.81 ($CF_3{-}$, 3F). Anal. Calcs. for ($C_{15}H_5O_4F_{15}$): C, 33.73%; H, 0.94%. Found: C, 34.10%; H, 1.08%.

Phenyl 4-(4-octanoyloxybenzoyloxy)benzoate (OBA oligomer model compound): OBA (1.3 g, 4.4 mmol) and 10 ml of thionyl chloride were placed into a flask equipped with a dropping funnel and a gas inlet tube. Several drops of *N*,*N*-dimethylformamide were added dropwise through the dropping funnel to this solution under a slow stream of nitrogen at 25 °C. Temperature was kept at 25 °C for 12 h. The excess of thionyl chloride was evaporated and then the product was extracted with hot *n*-hexane. Evaporation of *n*-hexane gave oily 4-octanoyloxybenzoyl chloride with the yield of 1.4 g (98%). Into a three-necked flask equipped with a dropping funnel, a thermometer and a gas inlet tube were placed phenyl 4-hydroxybenzoate (0.9 g, 4.4 mmol), triethylamine (0.5 g, 5.3 mmol) and 20 ml of dried tetrahydrofuran. Solution of 4-octanoyloxybenzoyl chloride (1.4 g, 4.4 mmol) in 10 ml of dried tetrahydrofuran was added dropwise through the dropping funnel under slow stream of nitrogen at 5 °C. Temperature was kept at 5 °C for 2 h and then at 25 °C for 12 h. The reaction mixture was filtrated to separate the triethylamine–HCl salts and acidified by diluted HCl solution. White precipitates were collected and washed with water. Recrystallization from ethyl acetate gave 1.7 g (77%) of phenyl 4-(4-octanoyloxybenzoyloxy)benzoate. Purity was checked by HPLC. Product characteristics were as follows. Tm: 107 °C. IR (KBr, cm^{-1}): 3070 (aromatic C–H), 2952, 2925, 2852 (aliphatic C–H), 1743 (ester C=O), 1732 (ester C=O). ^{1}H NMR ($CDCl_3$, ppm): $\delta = 0.75–0.92$ (t, CH_3–, 3H), 1.12–1.45 (m, $CH_3–(CH_2)_4$–, 8H), 1.61–1.80 (qnt, –CH_2–CH_2–COO–, 2H), 7.10–7.26 (m, aromatic, 5H), 7.27–7.44 (n, aromatic, 4H), 8.18 (d, aromatic 2H), 8.23 (d, aromatic 2H). Anal. Calcs. for ($C_{28}H_{28}O_6$): C, 73.03%; H, 6.13%. Found: C, 73.20%; H, 6.01%.

Phenyl 4-(4-perfluorooctanoyloxybenzoyloxy)benzoate (FOBA oligomer model compound): FOBA oligomer model compound was synthesized by the similar procedure. Product characteristics were as follows. Tm: 94 °C. IR (KBr, cm^{-1}): 3080 (aromatic C–H), 1245 (aliphatic C–F), 1785 (4-perfluorooctanoyloxy C=O), 1722 (phenyl ester C=O). ^{1}H NMR ($CDCl_3$, ppm): $\delta = 7.09–7.24$ (m, aromatic, 5H), 7.25–7.49 (m, aromatic, 4H), 8.20 (d, aromatic, 2H), 8.25 (d, aromatic, 2H). ^{19}F NMR ($CDCl_3$, ppm): $\delta = -121.43$ (CF_3–CF_2–, 2F), −118.03 (CF_3–CF_2–CF_2–, 2F), −117.64 (CF_3–CF_2–CF_2–CF_2–, 2F), −117.25 (CF_3–CF_2–CF_2–CF_2–CF_2–, 2F), −116.85 (CF_3–CF_2–CF_2–CF_2–CF_2–CF_2–, 2F), −113.44 (–CF_2–COO–, 2F), −76.07 (CF_3–, 3F). Anal. Calcs. for ($C_{28}H_{13}O_6F_{15}$): C, 46.05%; H, 1.79%. Found: C, 45.88%; H, 1.90%.

2.4. Polymerization

Polymerization of FOBA was described as a typical procedure. Into a cylindrical flask equipped with a mechanical stirrer and a gas inlet tube were placed FOBA (0.89 g, 1.66 mmol) and 20 ml of LPF. The reaction mixture was heated under slow stream of nitrogen up to 320 °C with stirring. Stirring was stopped when FOBA was entirely dissolved. The reaction temperature was kept at 320 °C. The solution became turbid and then the polymer was formed as precipitates after 6 h. Some of the FOBA sublimed during heating. The precipitates were collected by vacuum filtration at 320 °C and washed with *n*-hexane and acetone. Filtrate was poured into *n*-hexane and the precipitated oligomers which were dissolved in LPF at 320 °C were recovered by filtration. IR of precipitated polymer crystals (KBr, cm^{-1}): 3080 (aromatic C–H), 1741 (ester C=O), 1599, 1510, 1413 (1,4-phenylene C=C).

3. Results and discussion

3.1. Morphology of products

Various 4-acyloxybenzoic acids were synthesized and polymerized to clarify the influence of oligomer end-group on the morphology of POB. Polymerizations were carried out in LPF at 320 °C for 6 h with eliminating corresponding aliphatic acid. Polymerization concentration was 0.3–1.0% based on the polymer weight and the solvent volume. Polymerization results of PBA, HBA, OBA and DBA are presented in Table 1. Oligomers were not left in solution after 6 h and low yields of the polymers were due to the sublimation of monomers. All these monomers were insoluble in LPF at 25 °C but they were dissolved during heating up to 320 °C. Polymerization solutions became turbid within several minutes at 320 °C due to the precipitation of oligomers, and then the crystals grew gradually with the progress of polymerization. Fig. 1 shows the morphology of the obtained crystals. The needle-like or pillar-like crystals were obtained from these monomers, indicating that they were formed by the crystallization of oligomers. In contrast to this, the polymerization of FOBA yielded microspheres having needle-like crystals on the surfaces. The diameter of the microspheres was on the average 6 μm. The needle-like crystals appeared on the surface of the microspheres were approximately 1–2 μm in length and 0.1 μm in width. Lower polymerization concentration than 0.5% did not yield any polymer crystals. The microspheres formed at an initial stage in the polymerization did not possess needle-like crystals on the surface as discussed later and this spherical morphology strongly suggested that the microspheres were formed via liquid–liquid phase separation of oligomers as previously reported [21–23]. The microspheres were totally insoluble in organic solvents and useful measurements such as NMR and GPC could not be applied. The chemical structure of the microspheres was analyzed by IR spectra. The peak for C=O of ester group appeared newly at 1741 cm^{-1}. The characteristic peaks of FOBA such as C=O of perfluorooctanoyl group at 1785 cm^{-1}, C=O of carboxylic acid at 1700 cm^{-1}, –OH of carboxylic acid at 3300–2500 cm^{-1} and C–F of perfluorooctanoyl group at 1245 cm^{-1} disappeared. The spectrum is identical with that of POB. Fig. 2 shows the WAXS profiles of the microspheres prepared from FOBA. The characteristic peaks of the POB crystal [24] were clearly observed at 2θ of 19°, 21°, 24° and 28°. The diffraction peaks of the obtained microspheres having needle crystals were sharp and the diffuse halo attributed to amorphous part hardly existed. This pattern indicates that the microspheres possess high crystallinity.

Reaction-induced phase separation of oligomers in poor solvent is describable on a $C–T$ phase diagram analogous to that of partially miscible polymer–solvent system [25–27].

Table 1
Results of polymerization of various 4-acyloxybenzoic acids[a]

Run no.	Monomer code[b]	Polymerization concentration (%)	Yield of precipitates (%)	Morphology
1	PBA	1.00	29	Needle
2	HBA	1.00	30	Pillar
3		0.75	32	Needle
4	OBA	1.00	25	Pillar
5		0.30	21	Needle
6	DBA	1.00	65	Pillar
7		0.30	13	Needle
8	FOBA	1.00	27	Sphere needle[c]
9		0.75	7	Sphere needle
10		0.50	0	–

[a] Polymerizations were carried out at 320 °C in LPF for 6 h.
[b] Monomer codes are shown in Scheme 1.
[c] Sphere-needle stands for the microspheres having needle-like crystals on the surface.

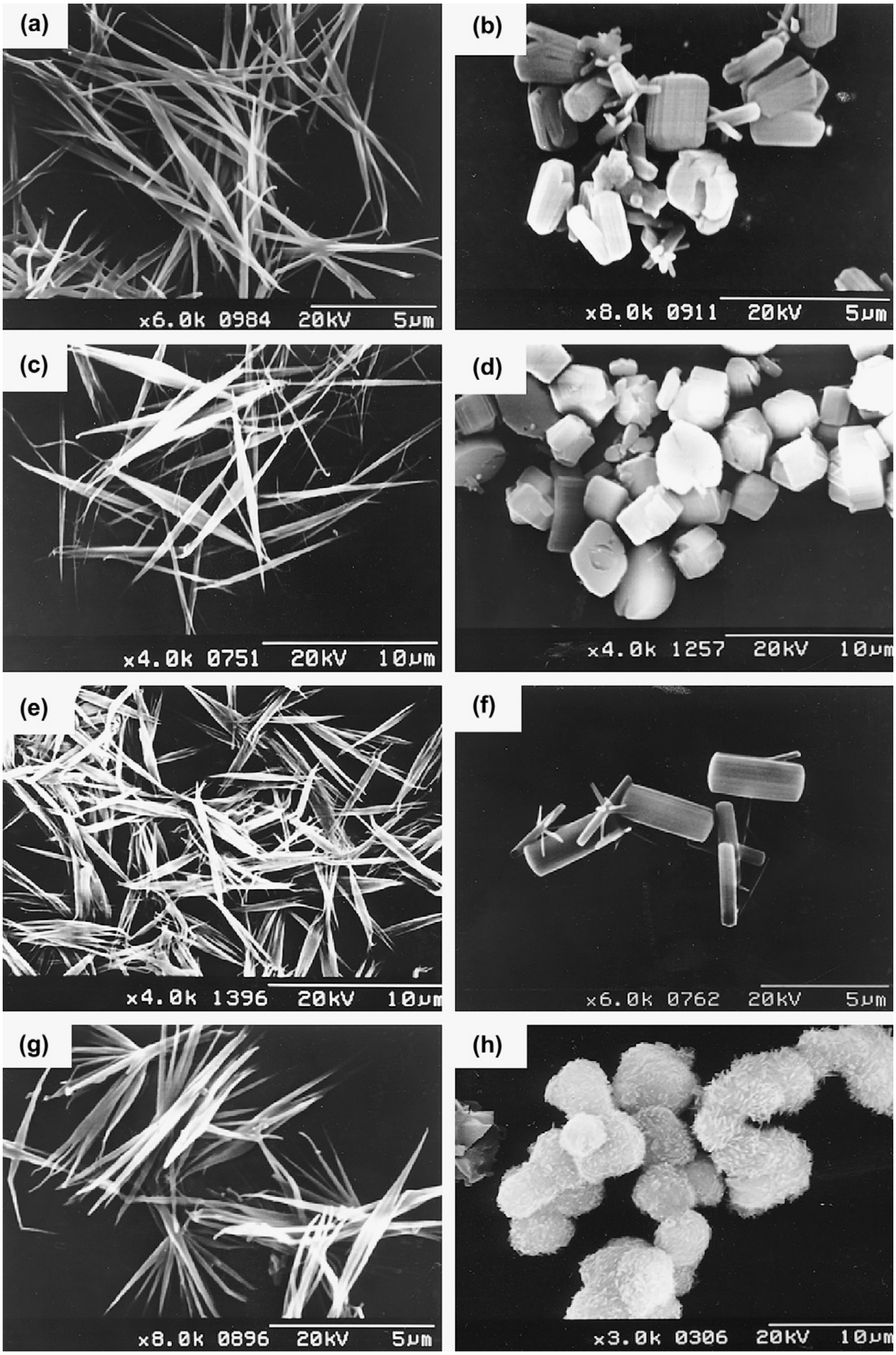

Fig. 1. POB crystals prepared in (a) run no. 1, (b) run no. 2, (c) run no. 3, (d) run no. 4, (e) run no. 5, (f) run no. 6, (g) run no. 7, and (h) POB microspheres having needle-like crystals on the surface prepared in run no. 8.

The phase-separation curve in the repulsive system, in which there is no attractive interaction between the oligomer and the solvent, can be written as a combination of a freezing point curve of the oligomers and an upper critical solution temperature (UCST) type consolution curve. Schematic phase diagram is illustrated in Fig. 3. $C-T$ phase diagrams of ABA, ABA dimer and ABA trimer in LPF were prepared by cloud point measurements to know the phase equilibrium described above. The phase-separation curves shown in Fig. 4 are combinations of freezing point curves of the compounds and UCST type consolution curves. Both the freezing point curve and the consolution curve shift toward higher temperature with

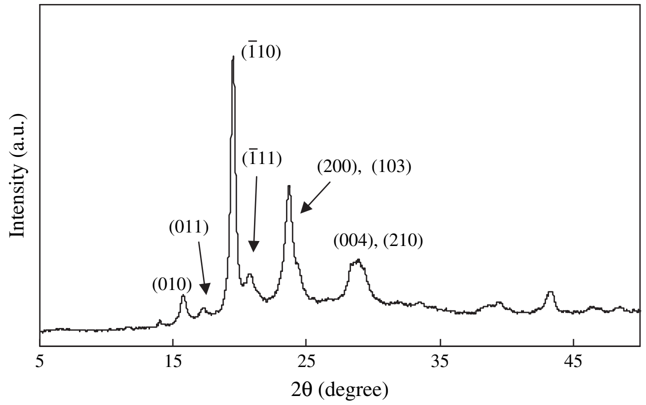

Fig. 2. WAXS profile of the microspheres having needle-like crystals on the surface prepared in run no. 8.

the increase in DPn. These compounds started to polymerize over 250 °C and thereby the phase diagrams at temperature higher than 250 °C could not be prepared. In the course of actual polymerization, DPn of oligomer dissolved in solution increases gradually with time. When the DPn of oligomer exceeds a critical value, oligomers are phase separated. If the supersaturated oligomers are precipitated across the freezing point curve, they are phase separated by crystallization to form polymer crystals. On the other hand, if the supersaturated oligomers are precipitated across the consolution curve, microdroplets are formed via liquid–liquid phase separation and then finally polymer microspheres are obtained. In order

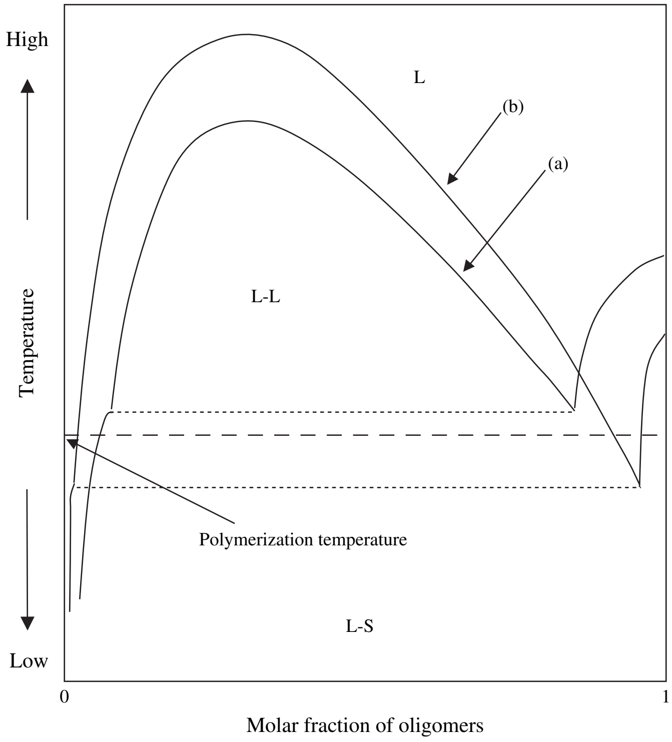

Fig. 3. Schematic drawing for C–T phase of partially miscible system of LPF and oligomers prepared from (a) PBA, HBA, OBA and DBA, and (b) FOBA. L: liquid phase, L–L: two immiscible liquids' phase, L–S: liquid and solid phases.

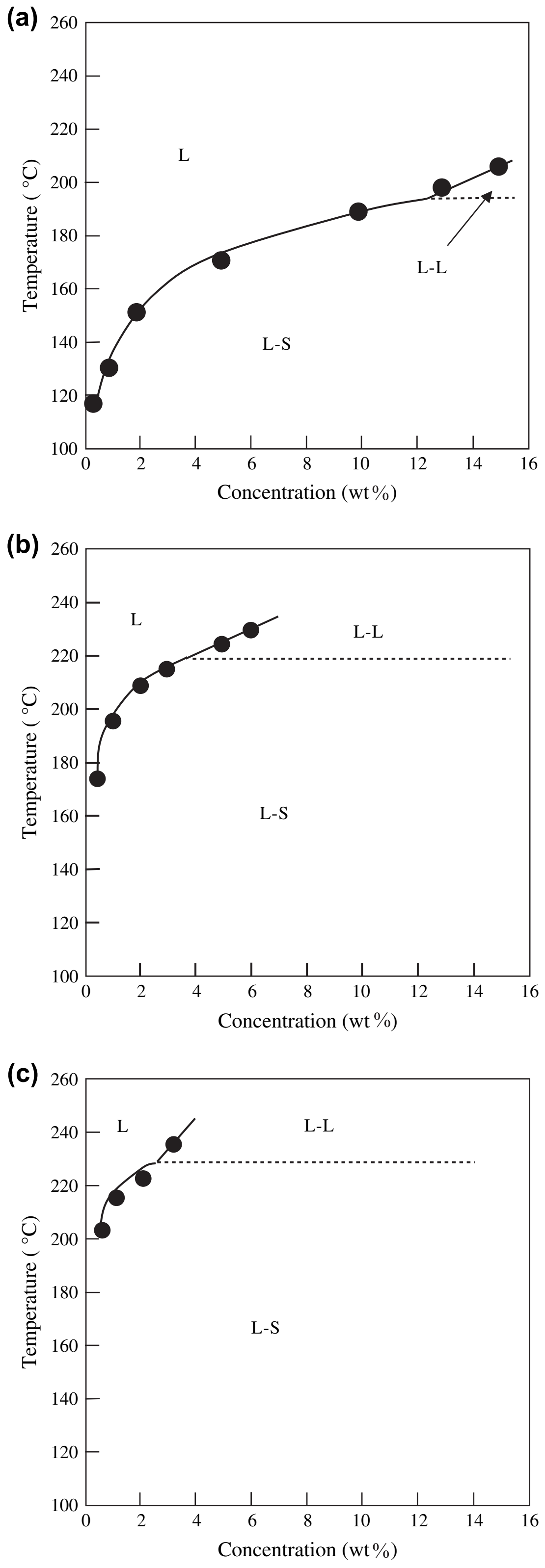

Fig. 4. C–T phase diagram for systems of LPF and (a) ABA, (b) ABA dimer and (c) ABA trimer. L: liquid phase, L–L: two immiscible liquids' phase, L–S: liquid and solid phases.

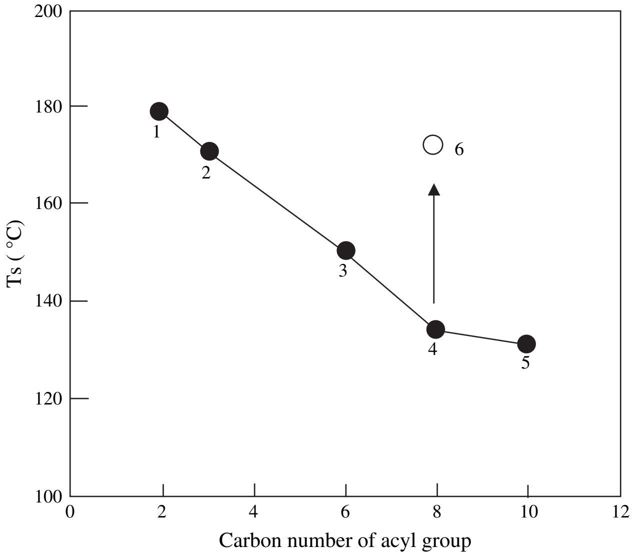

Fig. 5. Plot of T_s as a function of carbon number of acyl group in monomers. 1: ABA, 2: PBA, 3: HBA, 4: OBA, 5: DBA and 6: FOBA.

to understand the difference in the morphology of POB formed from FOBA and other monomers, relative location of the phase-separation curves in the polymerization system of FOBA was compared with that of OBA by division into the freezing point curve and the consolution curve. The oligomers were insoluble in common organic solvents under the temperature at which the polymerization began and hence the phase-separated oligomers could not be isolated. The consolution curve and the freezing point curve of the phase-separated oligomer could not be accurately determined. Temperature (Ts) at which the monomer was completely dissolved on heating could be adopted as a criterion to compare the miscibility of oligomer and LPF. The phase-separation curve was assumed from the data of Ts and DPn of the phase-separated oligomers. Fig. 5 plots Ts against the carbon number of acyl group in the monomers. The monomers having longer acyl groups showed lower Ts except for FOBA, and the longer acyl end-group enhanced miscibility between the oligomers and LPF. However, Ts of FOBA was 172 °C, which was 40 °C higher than OBA. The higher Ts indicated the lower miscibility between the oligomers derived from FOBA and LPF than that from OBA and LPF. This is due to the perfluorooctanoyl end-group, and the lower miscibility makes the consolution curve shift toward higher temperature on $C-T$ phase diagram. Oligomers were collected just before the polymerization solution became turbid to evaluate their DPns. The DPns of the oligomers generated from FOBA and OBA were 1.6 and 2.2, respectively. This result implies that lower molecular weight oligomers were phase separated in the polymerization of FOBA than OBA due to the lower miscibility. It is well known that the freezing point of oligomers is a function of DPn and that it increases with increasing DPn due to mainly decrease of entropy contribution for coagulation [28,29]. Hence, the lower DPn of the phase-separated oligomers prepared from FOBA makes the freezing point curve shift toward lower temperature. As a result of the shifts of both the consolution curve and the freezing point curve, two immiscible liquids' phase becomes wide on $C-T$ phase diagram in the polymerization system of FOBA, and hence the microspheres are formed from FOBA through a formation of microdroplets by liquid–liquid phase separation of oligomers. Phenyl 4-(4-octanoyloxybenzoyl)benzoate and phenyl 4-(4-perfluorooctanoyloxybenzoyl)benzoate were synthesized as OBA and FOBA oligomer model compound, and $C-T$ phase diagrams of these compounds and LPF were prepared. The consolution curve of FOBA oligomer model compound shifted toward higher temperature than OBA oligomer model compound as shown in Fig. 6. A boundary line between two immiscible liquids' phase and liquid–solid phases in FOBA oligomer model compound–LPF system was located at lower temperature than OBA oligomer model compound–LPF system. Then the resultant two immiscible liquids' phase was widely expanded substantiating above discussion.

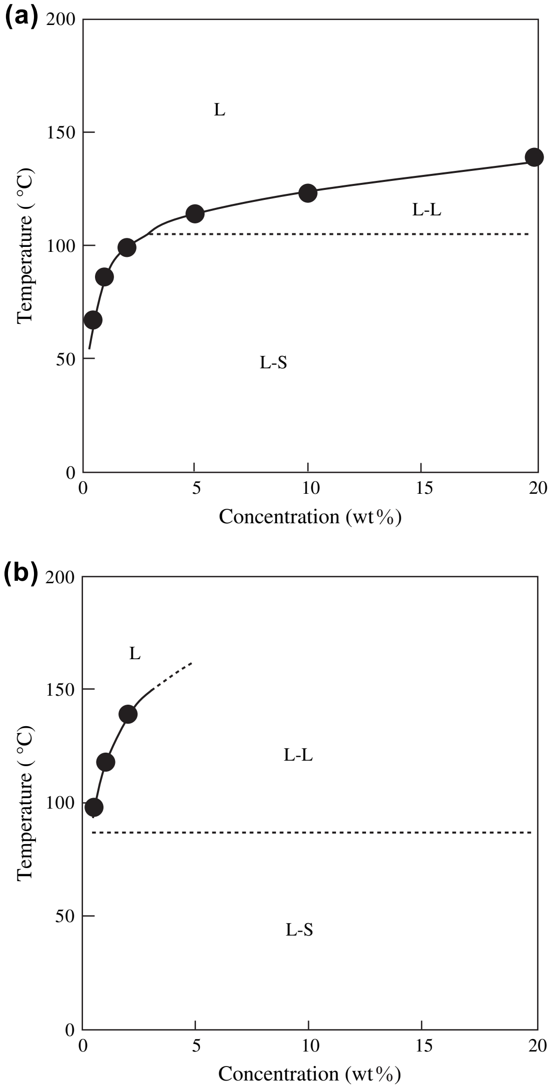

Fig. 6. $C-T$ phase diagram of (a) OBA oligomer model compound–LPF and (b) FOBA oligomer model compound–LPF.

3.2. Formation mechanism of microspheres having needle-like crystals

The microspheres prepared from FOBA have needle-like crystals on the surface. The yield of the microsphere and the recovery yield of the oligomer were plotted as a function of polymerization time as shown in Fig. 7. DPns of the microspheres and the dissolved oligomers recovered from the solution were also plotted in Fig. 7. The yield of the microsphere increased with time and the recovery yield of the oligomer decreased reversibly. This fact shows that the microspheres grew by consecutive supply of oligomers from liquid phase. The DPn of the polymers composed the microspheres increased with time owing to the further polymerization in the microdroplets in which the oligomer concentration was quite high. The increase in DPn causes the crystallization in the microdroplets leading the solidification and the microspheres having smooth surfaces are formed. The DPn of the dissolved oligomer increased gradually at the initial stage in the polymerization and then largely from 1.6 to 3.0 at around 2–3 h. Morphological change in microspheres was observed with time as shown in Fig. 8. Interestingly, the microspheres obtained at the initial stage in the polymerization had smooth surfaces and any needle-like crystals did not appear. The needle-like crystals appeared on the surface after 3 h and then they grew with time. The needle-like crystals appeared on the surface of the microspheres when the DPn of the dissolved oligomers increased largely. Concentration of oligomers dissolved in the solution decreases with polymerization time due to the precipitation of oligomers, resulting in making the critical DPn of the phase-separated oligomers higher. The increase in critical DPn makes the freezing point curve shift

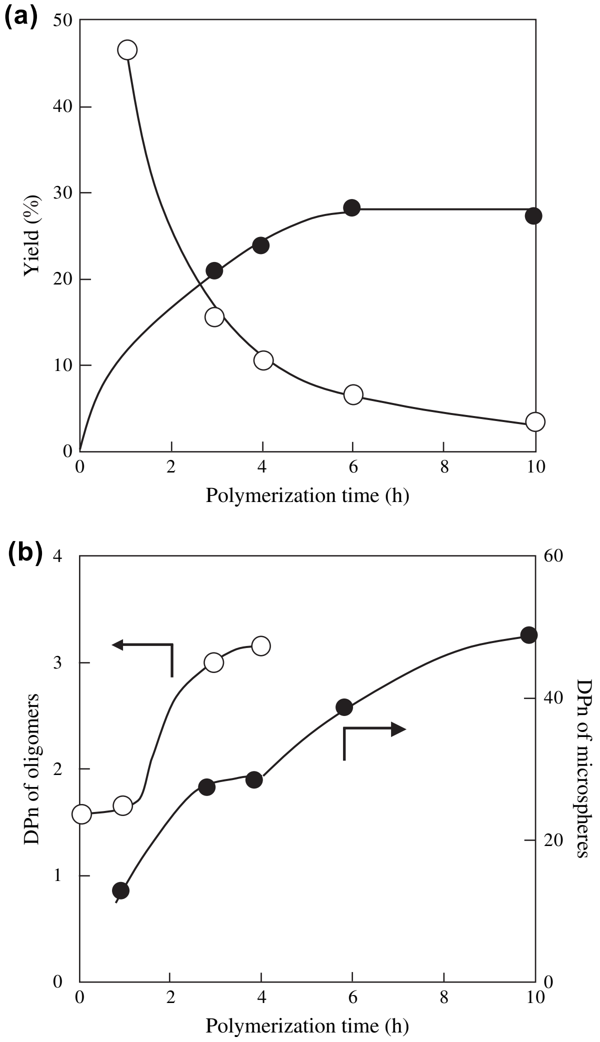

Fig. 7. Polymerization time dependencies of (a) yield and (b) DPn of (●) microsphere and (○) oligomer generated from FOBA.

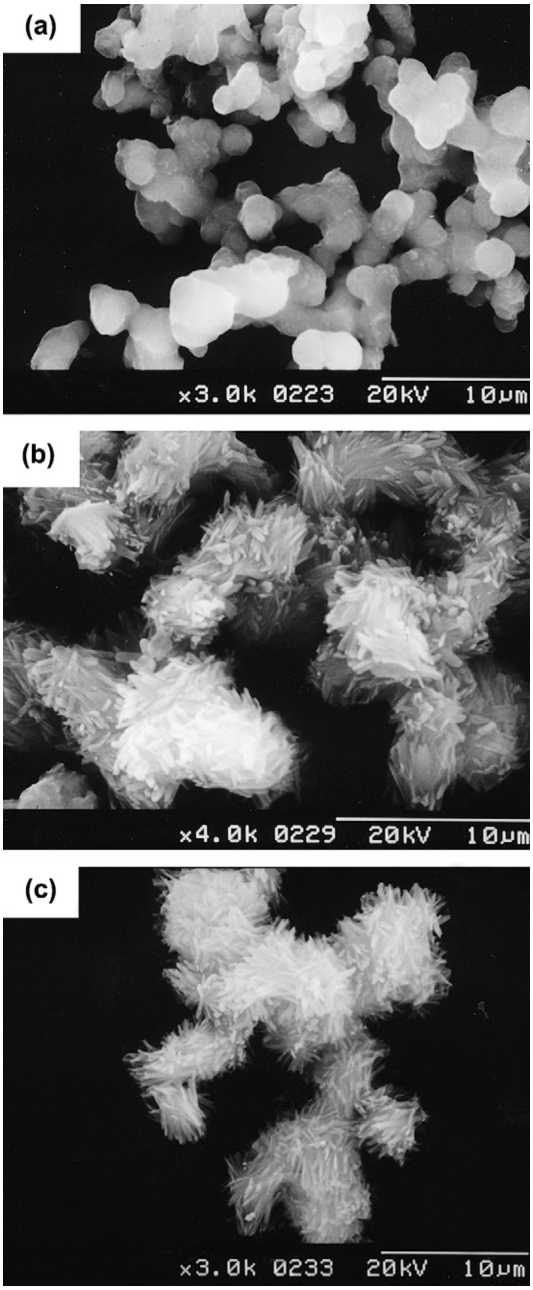

Fig. 8. Microspheres prepared from FOBA at 1.0% for (a) 1 h, (b) 4 h and (c) 10 h.

toward higher temperature on $C-T$ phase diagram and then the oligomers tend to precipitate across the freezing point curve on the surface of already formed microspheres. Phase-separation behaviour changes from liquid–liquid phase separation to crystallization at around 3 h and then the needle-like crystals appear on the surface of the microspheres by the heterogeneous nucleation. As shown in Fig. 7, the DPn curve of the microspheres exhibited an infliction point at 4 h, that is, the DPn of the microspheres was once leveled off at 3–4 h and then increased again after the yield was leveled off. Solid-state polymerization might occur more effectively in the needle-like crystals compared with the microspheres as reported previously [8,30], and the DPn increased continuously in needle-like crystals. The increase in the DPn after 4 h might be mainly caused by the solid-state polymerization in the needle-like crystals on the microspheres.

4. Conclusions

The polymerizations of PBA, HBA, OBA and DBA yielded needle-like or pillar-like POB crystals via the crystallization of oligomers. On the other hand, the polymerization of FOBA afforded microspheres having needle-like crystals on the surface. Perfluorooctanoyl end-group expanded liquid–liquid phase-separation region due to the lower miscibility and oligomers were phase separated via liquid–liquid phase separation to form the microspheres having smooth surface. Concentration of the dissolved oligomers in the solution decreased due to the phase separation of oligomers resulting in the increase in DPn of the phase-separated oligomer. Thereby the phase-separation behaviour of oligomers changed from liquid–liquid phase separation to crystallization during polymerization and the oligomers were crystallized to form needle-like crystals on the surface of the microspheres after middle stage of polymerization. The chemical structure of oligomer end groups strongly affected the phase-separation behaviour of oligomers.

Acknowledgements

This study was financially supported by Industrial Technology Research Grant Program in 2004 from New Energy and Industrial Technology Development Organization of Japan, and Strategic Solid Waste Management for Sustainable Society, Centre of Excellence Program for the 21st Century, Ministry of Education, Culture, Sports, Science and Technology, Japan.

References

[1] For examples: Cassidy PE. Thermally stable polymers, syntheses and properties. New York: Marcel Dekker; 1980;
Korshak VV. Heat-resistant polymers, Israel program for scientific translations. Jerusalem; 1971;
Seymour RB, Krishenbaum GS. High performance polymers: their origin and development. New York: Elsevier Science Publishing; 1986.
[2] Economy J, Nowak BE, Cottis SD. SAMPE J 1970;6:6.
[3] Economy J, Storm RS, Matkovick MI, Cottis SG, Novak BE. J Polym Sci Polym Chem 1976;14:2207.
[4] Economy J, Volksen W, Geiss R. Mol Cryst Liq Cryst 1984;105:289.
[5] Economy J, Volksen W, Viney C, Geiss R, Siements R, Karis T. Macromolecules 1988;21:2777.
[6] Kricheldorf HR, Schwarz G. Polymer 1984;25:520.
[7] Liezer G, Schwarz G, Kricheldorf HR. J Polym Sci Polym Phys 1983;21:1599.
[8] Yamashita Y, Kimura K. Polymeric materials encyclopedia. Boca Raton, FL: CRC Press; 1996. p. 8707.
[9] Yamashita Y, Kato Y, Endo S, Kimura K. Makromol Chem Rapid Commun 1988;9:687.
[10] Kimura K, Endo S, Kato Y, Yamashita Y. Polymer 1993;35:123.
[11] Kimura K, Yamashita Y. Polymer 1994;35:3311.
[12] Kimura K, Endo S, Kato Y, Yamashita Y. Polymer 1993;34:1054.
[13] Kricheldorf HR, Schwarz G, Ruhser F. Macromolecules 1991;24:3485.
[14] Kricheldorf HR, Struve O, Schwarz G. Polymer 1996;37:4311.
[15] Kricheldorf HR, Schwarz G, Adebahr T, Wilson DJ. Macromolecules 1993;26:6622.
[16] Schwarz G, Kricheldorf HR. Macromolecules 1995;28:3911.
[17] Mencsel J, Walsh JP, Wunderlich B. J Polym Sci Polym Phys 1981;19:837.
[18] Neubert ME, Colby C, Ezenyilimba MC, Jorousek MR, Leonhardt D, Leung K. Mol Cryst Liq Cryst 1988;154:127.
[19] Tsonev LV, Petrov MP, Barbero G. Liq Cryst 1988;24:853.
[20] Kobashi K, Kimura K, Yamashita Y. Polymer 2004;45:7099.
[21] Kimura K, Yokoyama F, Yamashita Y. Preprints, IUPAC World Polymer Congress, 37th international symposium on macromolecules; 1998. p. 574.
[22] Kimura K, Ohmori H, Yokoyama F, Yamashita Y. Polym Prepr ACS 1998;39:863.
[23] Kimura K, Yamashita Y. Extended abstracts. 14th annual meeting PPS-14; 1998. p. 577.
[24] Yamashita Y, Nishimura S, Fujiwara H, Monobe K, Shimamura K. Polym Prepr Jpn 1983;32:2589.
[25] Richards RB. Trans Faraday Soc 1946;42:10.
[26] Flory PJ, Mandelkern L, Hall HK. J Am Chem Soc 1951;73:2532.
[27] Koningsveld R, Stochmayer WH, Nies E. Polymer phase diagrams. New York: Oxford University Press; 2001.
[28] Mita I, Yokota R, Kambe H. Rep Prog Polym Phys Jpn 1971;16:319.
[29] Kojima Y, Ichinose K, Nakamura T, Hosaka N. Kobunshi Ronbunshu 1978;35:629;
Chem Abstr 1979;90:39392n.
[30] Kimura K, Inoue H, Kohama S, Yamashita Y, Sakaguchi Y. Macromolecules 2003;36:7721.